

# NEURALKALMAN: A LEARNABLE KALMAN FILTER FOR ACOUSTIC ECHO CANCELLATION

Yixuan Zhang<sup>1,2,\*</sup>, Meng Yu<sup>1</sup>, Hao Zhang<sup>1</sup>, Dong Yu<sup>1</sup>, DeLiang Wang<sup>2</sup>

<sup>1</sup>Tencent AI Lab, Bellevue, WA, USA

<sup>2</sup>The Ohio State University, Columbus, OH, USA

## ABSTRACT

The Kalman filter is widely used for addressing acoustic echo cancellation (AEC) problems due to their robustness to double-talk and fast convergence. However, the inability to model nonlinearity and the need to tune control parameters cast limitations on such adaptive filtering algorithms. In this paper, we integrate the frequency domain Kalman filter (FDKF) and deep neural networks (DNNs) into a hybrid method, called NeuralKalman, to leverage the advantages of deep learning and adaptive filtering algorithms. Specifically, we employ a DNN to estimate nonlinearly distorted far-end signals, a transition factor, and the nonlinear transition function in the state equation of the FDKF algorithm. Experimental results show that the proposed NeuralKalman improves the performance of FDKF significantly and outperforms strong baseline methods.

**Index Terms**— Acoustic echo cancellation, Kalman filter, deep learning, NeuralKalman

## 1. INTRODUCTION

Acoustic echo cancellation (AEC), as an active and challenging research problem in the domain of speech processing, has been studied for decades and is widely used in mobile communication and teleconferencing systems. The goal of AEC is to eliminate the far-end signal from the near-end microphone signal so as to remove the echo of the far-end signal (back to the far end). In conventional digital signal processing (DSP) based adaptive filtering algorithms such as normalized least mean square (NLMS) and affine projection [1, 2, 3], RLS [4], echo removal is achieved by constantly estimating the linear transfer function between the loudspeaker playing the far-end signal and the near-end microphone, known as the echo path. However, in such AEC algorithms, control parameters need to be tuned to ensure fast convergence, and nonlinearity modeling (i.e. nonlinearity introduced by a loudspeaker) is missing.

With recent advances in deep neural networks, deep learning-based methods [5, 6, 7] have been utilized for AEC, and their ability to model nonlinear relations leads to promising results, even in challenging noisy or double-talk scenarios. Such methods usually treat AEC as a source separation problem and directly estimate the near-end signal based on the microphone and far-end reference signal. While achieving good performance in general, DNN-based methods have shown limited utility in dealing with continuously changing echo paths [8]. In recent AEC challenges [9], two-stage hybrid systems [10, 11, 12] that use DNN as a nonlinear post-processor of a DSP-based adaptive filtering algorithm have shown promising results. In such hybrid systems, DNNs perform nonlinear residual echo suppression, which compensates for the drawbacks of adaptive

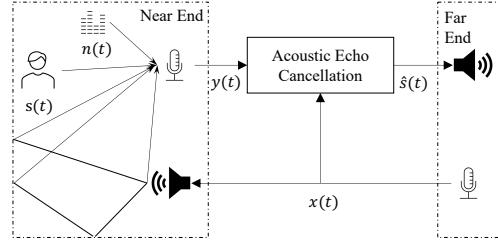


Fig. 1: An acoustic echo scenario with background noise.

filtering algorithms. To further leverage the advantages of DNN and adaptive filtering algorithms, methods such as Deep Adaptive AEC [8] train DNNs where a linear adaptive algorithm is embedded as differentiable layers. Such a hybrid system has shown superior results in modeling a continuously changing echo path compared to DNN-based and two-stage hybrid methods.

As an adaptive filtering algorithm for AEC, the frequency domain Kalman filter (FDKF) [13, 14] shows robustness in double-talk scenarios and better convergence rates. Hybrid methods based on the Kalman filter algorithm have been used in research fields [15, 16, 17] such as pose estimation, and speech filtering, but have not been well explored in the domain of AEC. The most related study is the Neural Kalman Filtering proposed in [18], where a DNN is trained to estimate a Kalman gain. However, this method omits steps in the Kalman filter and results in a model similar to an NLMS-based hybrid method that does not fully take advantage of the Kalman filter. Hence whether DNN can improve Kalman filter-based AEC remains an open question.

In this study, we aim to improve the frequency-domain Kalman filtering algorithms through deep learning in several aspects. We find that simply replacing components in the Kalman filter does not always lead to better performance, but estimating missing or approximated components can bring improvements. Specifically, we utilize DNN to estimate the nonlinearly distorted far-end signal, a transition factor, and the nonlinear transition function in the state equation of the frequency-domain Kalman filter. Experimental results show that modeling the nonlinear distortion in far-end signals yields substantial improvements to the NeuralKalman. The transition factor shows adaptations to abrupt echo path changes and introducing a nonlinear transition function in the state equation accelerates training. Compared to modeling the covariance of the state noise and observation noise, we observe that injecting a nonlinear transition function in the state equation achieves similar improvement with less computation. The results show that the proposed hybrid NeuralKalman model suppresses echo well and outperforms the recent NLMS-based Deep Adaptive AEC [8].

\*This work was done during an internship at Tencent AI Lab.

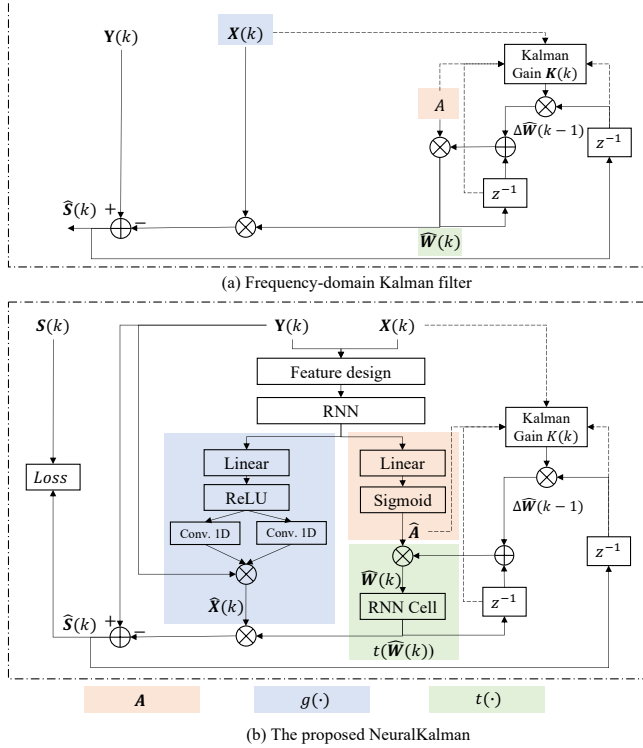


Fig. 2: Diagrams of (a) Frequency-domain Kalman filter and (b) proposed NeuralKalman, where  $z^{-1}$  denotes the unit delay.

## 2. PROPOSED METHOD: NEURALKALMAN

A typical acoustic echo scenario with background noise is shown in Fig. 1. The far-end signal  $x(t)$  is transmitted to the near end via a loudspeaker and received by a microphone as acoustic echo  $d(t)$ :

$$d(t) = h(t) * NL(x(t)) \quad (1)$$

where  $h(t)$  represents the echo path,  $NL(\cdot)$  represents the nonlinear distortion from the loudspeaker,  $*$  denotes convolution. The microphone signal  $y(t)$  is composed of echo  $d(t)$ , near-end speech  $s(t)$  and noise  $n(t)$ :

$$y(t) = s(t) + n(t) + d(t) \quad (2)$$

and it is usually processed, with the far-end signal  $x(t)$  as a reference, for echo removal before being sent to the far end.

### 2.1. Frequency-domain Kalman Filter

Frequency-domain Kalman filter for AEC [13, 14] estimates echo signal by modeling the echo path with an adaptive filter  $\hat{\mathbf{W}}(k)$  where  $k$  denotes the frame index, as shown in Fig. 2(a). In this study, we focus on AEC in clean condition and aim at estimating the near-end speech  $s(t)$ . FDKF can be interpreted as a two-step procedure (prediction and updating) and the updating of filter weights is achieved through the iterative feedback from the two steps. In the prediction step, the near-end signal  $\hat{\mathbf{S}}(k)$  is estimated by the measurement equation,

$$\hat{\mathbf{S}}(k) = \mathbf{Y}(k) - \mathbf{X}(k)\hat{\mathbf{W}}(k), \quad (3)$$

where  $\hat{\mathbf{S}}(k)$ ,  $\mathbf{Y}(k)$ , and  $\mathbf{X}(k)$  are the short-time Fourier transform (STFT) of the target speech, microphone, and far-end signal respectively. Inverse STFT is applied on  $\hat{\mathbf{S}}(k)$  to obtain the time-domain

$\hat{s}(t)$  as well.  $\hat{\mathbf{W}}(k)$  denotes the estimated echo path in the frequency domain. In the update step, the state equation for updating echo path  $\hat{\mathbf{W}}(k)$  is defined as,

$$\hat{\mathbf{W}}(k+1) = A[\hat{\mathbf{W}}(k) + \mathbf{K}(k)\hat{\mathbf{S}}(k)], \quad (4)$$

where  $A$  is the transition factor.  $\mathbf{K}(k)$  denotes the Kalman gain. As shown in Fig. 2(a),  $\mathbf{K}(k)$  is related to far-end signal  $\mathbf{X}(k)$ , echo path  $\hat{\mathbf{W}}(k-1)$  and estimated near-end signal  $\hat{\mathbf{S}}(k-1)$ . The dash line indicates indirect relations. The calculation of  $\mathbf{K}(k)$  is defined as,

$$\mathbf{K}(k) = \mathbf{P}(k)\mathbf{X}^H(k)[\mathbf{X}(k)\mathbf{P}(k)\mathbf{X}^H(k) + 2\Psi_{vv}(k)]^{-1}, \quad (5)$$

$$\mathbf{P}(k+1) = A^2[\mathbf{I} - \frac{1}{2}\mathbf{K}(k)\mathbf{X}(k)]\mathbf{P}(k) + \Psi_{\Delta\Delta}(k), \quad (6)$$

where  $\mathbf{P}(k)$  is the state estimation error covariance.  $\Psi_{vv}(k)$  and  $\Psi_{\Delta\Delta}(k)$  are observation noise covariance and process noise covariance respectively and are approximated by the covariance of the estimated near-end signal  $\Psi_{\hat{s}\hat{s}}(k)$  and the echo-path  $\Psi_{\hat{W}\hat{W}}(k)$ , respectively. More details can be found in [13].

### 2.2. NeuralKalman Framework

While being robust to double-talk and achieving a better convergence rate, the FDKF algorithm still faces several challenges. First, in the FDKF algorithm, the transition factor  $A$  in state equation Eq. 4 is set to a constant whose value is manually tuned according to the intensity of the echo path change variability. A fixed  $A$  is less likely to adapt well to the changing environment. Second, the echo is modeled as a linear transform of far-end signal  $\mathbf{X}(k)$  while neglecting the nonlinear distortion caused by amplifiers. Third, a linear relationship assumption is used in the updating of Kalman filter weights, as shown in the state equation Eq. 4. It is expected that using a nonlinear transition function in the estimation of echo path could help solve nonlinear AEC problems. To address these challenges, we introduce NeuralKalman framework, where the DNNs are employed to estimate the transition factor  $A$ , the far-end nonlinear distortion  $g(\cdot)$  and nonlinear transition function  $t(\cdot)$  for state equation (Eq. 4). The framework of the proposed NeuralKalman is depicted in Fig. 2(b).

#### 2.2.1. Transition Factor $A$

Transition factor  $A$  in the range of [0,1] depicts the variation of the Kalman filter and it is often manually tuned to a value that is close to 1. To incorporate the influence of possible echo path changing to transition factor, rather than using a fixed value, we employ DNN to estimate a time-varying transition factor for Eq. 4. Since the echo path and nonlinear distortion information can be retrieved from the microphone and far-end signals, in NeuralKalman, the input feature computed from the complex STFT of the microphone signal and far-end signal is shared for estimating transition factor  $A$  and nonlinear distortion  $g(\cdot)$ . Similar to NeuralEcho [7], the employed input feature is a concatenation of temporal correlation, frequency correlation, channel covariance, and normalized log power spectrum of microphone and far-end signal. As shown in Fig. 2(b), a recurrent neural network (RNN) takes the computed input feature and is followed by two branches for estimating nonlinearly distorted far-end signal  $\hat{\mathbf{X}}(k)$  and transition factor  $\hat{A}(k)$  respectively. The RNN is a 4-layer long short-term memory (LSTM) network where each layer has 257 hidden units. The branch for estimating frame-based transition factor  $\hat{A}(k)$  is composed of a linear layer followed by a sigmoidal activation function.

### 2.2.2. Nonlinear Distortion $g(\cdot)$

To address the nonlinear distortion introduced by the loudspeaker, we estimate the far-end nonlinear distortion with DNNs and use the nonlinear far-end signal as a reference for updating the Kalman filter. The nonlinearly distorted far-end signal  $\hat{\mathbf{X}}(k)$  is obtained by applying the complex-valued ratio filters  $cRF$  [19, 7] estimated from two one-dimensional convolution layers (Conv. 1D) to the microphone signal  $\mathbf{Y}(k)$ .

### 2.2.3. Nonlinear Transition Function $t(\cdot)$

To further address the nonlinear AEC problem and incorporate non-linearity in the estimation of echo path, we modify Eq. 4 by changing the linear transition function to a nonlinear one:

$$\hat{\mathbf{W}}(k+1) = t(A[\hat{\mathbf{W}}(k) + \mathbf{K}(k)\hat{\mathbf{S}}(k)]), \quad (7)$$

where the nonlinear transition function  $t(\cdot)$  is estimated from an LSTM cell which has 256 hidden units. The LSTM cell is trained using  $\hat{\mathbf{W}}(k)$  from Eq. 4 and previous state  $h_{k-1}$  as inputs. Then two linear layer takes  $h_k$  as input and outputs the real and imaginary parts of the processed  $t(\hat{\mathbf{W}}(k))$ .

$$\begin{aligned} h_k &= \mathbf{RNN}(\hat{\mathbf{W}}(k), h_{k-1}), \\ t(\hat{\mathbf{W}}(k)) &= \mathbf{FNN}(h_k), \end{aligned} \quad (8)$$

where  $\mathbf{RNN}$  and  $\mathbf{FNN}$  denote the LSTM cell and linear layers respectively.

### 2.2.4. Loss Function

The loss function is defined to simultaneously optimize SI-SDR [20] in the time domain and mean absolute error (MAE) of magnitude spectrogram between the target and estimated near-end signal.

$$L = -\mathbf{SISDR}(s, \hat{s}) + \alpha \mathbf{MAE}(|\mathbf{S}|, |\hat{\mathbf{S}}|), \quad (9)$$

where  $\hat{\mathbf{S}}$  and  $\hat{s}$  are the estimated frequency-domain and time-domain near-end signal, respectively. And  $\alpha$  in our implementation is set to 10000 to balance the value range of the two losses.

## 3. EXPERIMENTAL SETUP

### 3.1. Dataset

Following the experimental setup in [7], we generate the single-channel AEC dataset for training and testing using AISHELL-2 [21] and AEC-Challenge [9] datasets. We use clean far-end signals from AEC-Challenge’s synthetic echo set [9]. The far-end signals are nonlinearly distorted. Nonlinear distortions such as maximum amplitude clipping with a Sigmoidal function [5], learned distortion functions, etc. are included. To simulate acoustic echo, 10K room impulse responses (RIRs) sets with random room characteristics are generated using the image-source method [22] with reverberation time (RT60) ranging from 0 to 0.6 seconds. Each of the 10K RIRs sets comprises the RIRs from locations of the loudspeaker, near-end speaker. During data generation, the signal-to-echo-ratio (SER) ranges from -10 dB to 10 dB and RIRs set is randomly picked. The training set has 90K utterances, and 10K utterances are randomly selected in each epoch for training. Each network is trained for 90 epochs. We generated 200 utterances for validation and 300 utterances for testing. All input audios are sampled at 16 kHz. STFT is computed with a 32 ms frame length and 50% frame shift.

**Table 1:** Performance of NeuralKalman with various settings in the presence of double-talk.

	PESQ	WER (%)	ERLE (dB)
Unprocessed	1.87	79.85%	-
Kalman Filter [14]	2.32	32.89%	4.82
NeuralKalman-A	2.32	31.67%	4.95
NeuralKalman-A/ $g(\cdot)$	2.57	22.37%	30.73
NeuralKalman-A/ $g(\cdot)$ / $\Psi$	2.65	21.79%	<b>33.44</b>
NeuralKalman-A/ $g(\cdot)$ / $t(\cdot)$	<b>2.67</b>	<b>20.41%</b>	33.37

### 3.2. Evaluation Metrics

We evaluate the echo cancellation performance of the proposed NeuralKalman with three metrics including echo return loss enhancement (ERLE) [23], perceptual evaluation of speech quality (PESQ) [24] and word error rate (WER). ERLE (in dB) measures the extent of echo suppression and it is defined as

$$ERLE = 10 \log_{10} \left( \frac{\sum_t y(t)^2}{\sum_t \hat{s}(t)^2} \right), \quad (10)$$

PESQ is used to measure speech quality. For ERLE and PESQ, a higher value indicates better performance. To evaluate WER, we use a general-purpose mandarin speech recognition Tencent API [25] to test the automatic speech recognition (ASR) performance.

## 4. EXPERIMENTAL RESULTS

### 4.1. NeuralKalman Evaluation

We conduct an ablation study to investigate the influence of modeling transition factor  $A$ , nonlinear distortion  $g(\cdot)$  and nonlinear transition function  $t(\cdot)$ . NeuralKalman with different DNN components is built for comparison and the results are shown in Table 1. NeuralKalman-A refers to the model that employs DNN only for estimating the transition factor  $A$ . NeuralKalman-A/ $g(\cdot)$  uses DNN to jointly estimate the transition factor  $A$  and a nonlinear distortion function  $g(\cdot)$ . NeuralKalman-A/ $g(\cdot)$ / $t(\cdot)$  includes an additional RNN cell for estimating nonlinear transition function  $t(\cdot)$ . Details about the network structure are described in Sec. 2.2. In addition, since an accurate estimation of covariance matrices in FDKF would contribute to better convergence rate and AEC performance [13], we also train a NeuralKalman-A/ $g(\cdot)$ / $\Psi$  model with the covariance  $\Psi_{vv}(k)$  and  $\Psi_{\Delta\Delta}(k)$  learnt using LSTM cells with 256 hidden units. The inputs to the RNNs for estimating  $\Psi_{vv}(k)$  and  $\Psi_{\Delta\Delta}(k)$  are the estimated near-end speech  $\hat{\mathbf{S}}(k)$  and updated  $\hat{\mathbf{W}}(k)$ , respectively.

#### 4.1.1. Transition Factor $A$

In our implementation of the traditional Kalman filter, the optimal value we find for  $A$  that best fits the test set is 0.9995. However, it is more proper to use a time-varying  $A$  in scenarios with echo path changes to make the updating of the algorithm stable and diminish the chances of divergence. We plot the value of learned  $A$  from the NeuralKalman-A model on audios with and without abrupt echo path change in Fig. 3. It is observed that for the audio signal without echo path change, the learned  $A$  is close to 1 and relatively fixed throughout time. That explains why the performance of NeuralKalman-A is similar to that of FDKF. For the signal with abrupt echo path change, we observe that the value of learned  $A$

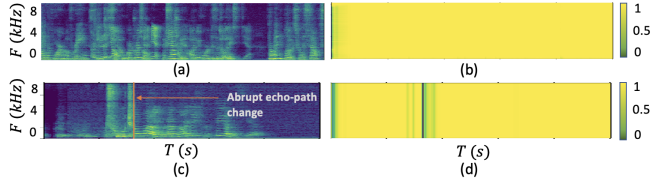


**Fig. 3:** Estimated transition factor  $A$  for signals with no echo path change (a, b) and with abrupt echo path change (c, d): (a)(c) Magnitude STFT of a microphone signal, (b)(d) Estimation of  $A$  from NeuralKalman- $A$  model.

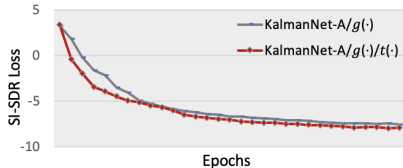


**Fig. 4:** SI-SDR loss curve of NeuralKalman- $A/g(\cdot)$  and NeuralKalman- $A/g(\cdot)/t(\cdot)$ .

decreases to nearly 0 when the echo path abruptly changes and gradually increases afterward, which is reasonable to obtain a stable convergence of the Kalman filter.

#### 4.1.2. Nonlinear Distortion $g(\cdot)$

While NeuralKalman- $A$  that models transition factor  $A$  gives Kalman filter flexibility to handle echo path changes and brings slight improvements in terms of WER, we observe that the key improvement comes from modeling the far-end nonlinear distortion. After further introducing far-end nonlinear distortion  $g(\cdot)$ , we observe that compared to NeuralKalman- $A$ , PESQ is increased by 0.25, ERLE is increased to 30.73, and WER is relatively reduced by 29.4%.

#### 4.1.3. Nonlinear Transition Function $t(\cdot)$

With the learned nonlinear transition function  $t(\cdot)$ , the performance of NeuralKalman is further improved. As shown in Table 1, PESQ is improved by 0.1, ERLE is improved by 2.64, and WER is relatively reduced by 8.8% compared to NeuralKalman- $A/g(\cdot)$ . In addition, we observe from Fig. 4 that estimating the nonlinear transition function  $t(\cdot)$  brings faster training convergence speed. By substituting approximated  $\Psi_{vv}(k)$  and  $\Psi_{\Delta\Delta}(k)$  in FDKF with DNN learned covariance, NeuralKalman- $A/g(\cdot)/\Psi$  has improved performance in terms of all metrics. Compared to NeuralKalman- $A/g(\cdot)/\Psi$ , we observe that NeuralKalman- $A/g(\cdot)/t(\cdot)$  can achieve slightly better performance with less computational cost so we decide to only estimate  $t(\cdot)$  instead of  $\Psi$ . Since that the transition factor  $A$  and nonlinear transition function  $t(\cdot)$  are both for tuning the state equation Eq. 4, we validate the necessity of estimating transition factor  $A$  by training a NeuralKalman- $g(\cdot)/t(\cdot)$  model where the estimation of  $A$  is eliminated. We observe that PESQ reduces by 0.1 and WER increases to 21.98%. The results indicate that estimating transition factor  $A$  is necessary.

**Table 2:** Performance comparison with baseline methods.

	PESQ	ERLE (dB)	WER (%)
Unprocessed	1.87	-	79.85%
Kalman Filter [14]	2.32	4.82	32.89%
NLMSNet [8]	2.52	28.14	23.33%
DNN-AEC	2.62	<b>33.68</b>	23.14%
NeuralKalman- $A/g(\cdot)/t(\cdot)$	<b>2.67</b>	33.37	<b>20.41%</b>

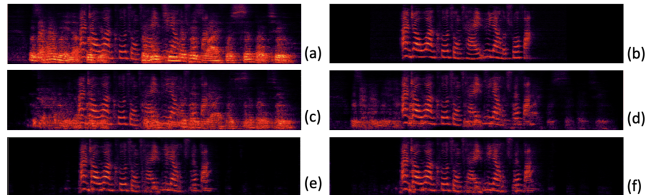


**Fig. 5:** Spectrograms of (a) microphone signal, (b) target near-end signal, and outputs of (c) Kalman filter, (d) NLMSNet, (e) DNN-AEC, and (f) our proposed method, NeuralKalman- $A/g(\cdot)/t(\cdot)$ .

## 4.2. Comparison with Baselines

We compare the proposed NeuralKalman- $A/g(\cdot)/t(\cdot)$  model with baseline methods including frequency-domain Kalman filter, a hybrid method of deep learning and NLMS (denoted as NLMSNet) [8], and a fully DNN-based model DNN-AEC. For a fair comparison, we utilize the same network structure for all the DNN-based methods. Comparison results are shown in Table 2. From the results, we observe that both hybrid methods including Deep Adaptive AEC and NeuralKalman- $A/g(\cdot)/t(\cdot)$  outperform the frequency domain Kalman filter algorithm. Compared with NLMSNet, NeuralKalman improves the PESQ by 0.15. WER is improved relatively by 12.5%. NeuralKalman gets comparable results with the DNN-AEC method in terms of ERLE and better PESQ and ASR performance. The PESQ is improved by 0.05 and WER is relatively improved by 11.8%. The results presented in [8] show that NLMSNet substantially outperforms the fully DNN-based method, which is different from what we obtained here. The major reason is that the signals used for training and testing in [8] are recorded in scenarios with continuous echo path changing, which helps show the benefits of using hybrid methods. Fig. 5 shows the magnitude STFT of the near-end signal estimated by different methods. Compared with other baseline methods, NeuralKalman- $A/g(\cdot)/t(\cdot)$  removes the echo more thoroughly.

## 5. CONCLUSION

In this paper, we have proposed a learnable Kalman filter for acoustic echo cancellation. The proposed model leverages the advantages of DNN to improve the Kalman filter by estimating the missing or approximated components, including the transition factor, nonlinear distortion of the far-end signal, and nonlinear transition function for the estimated echo path. Systematic evaluations show that the proposed method outperforms recent baseline methods. For future work, we will evaluate the performance of NeuralKalman using real-recorded signals with echo path changes and explore utilizing it in real-world devices.

## 6. REFERENCES

- [1] Donald L Duttweiler, "Proportionate normalized least-squares adaptation in echo cancelers," *IEEE Transactions on Speech and Audio Processing*, vol. 8, pp. 508–518, 2000.
- [2] Steven L Gay, "The fast affine projection algorithm," in *Acoustic Signal processing for Telecommunication*, pp. 23–45. 2000.
- [3] Andreas Mader, Henning Puder, and Gerhard Uwe Schmidt, "Step-size control for acoustic echo cancellation filters—an overview," *Signal Processing*, vol. 80, pp. 1697–1719, 2000.
- [4] Jafar Ramadhan Mohammed and Gurnam Singh, "An efficient RLS algorithm for output-error adaptive IIR filtering and its application to acoustic echo cancellation," in *IEEE Symposium on Computational Intelligence in Image and Signal Processing*, 2007, pp. 139–145.
- [5] Hao Zhang and DeLiang Wang, "Deep learning for acoustic echo cancellation in noisy and double-talk scenarios," in *Proc. Interspeech*, 2018, p. 322.
- [6] Hao Zhang and DeLiang Wang, "Neural cascade architecture for multi-channel acoustic echo suppression," *IEEE/ACM Transactions on Audio, Speech, and Language Processing*, vol. 30, pp. 2326–2336, 2022.
- [7] Meng Yu, Yong Xu, Chunlei Zhang, Shi-Xiong Zhang, and Dong Yu, "NeuralEcho: A self-attentive recurrent neural network for unified acoustic echo suppression and speech enhancement," *arXiv preprint arXiv:2205.10401*, 2022.
- [8] Hao Zhang, Srivatsan Kandadai, Harsha Rao, Minje Kim, Tarun Pruthi, and Trausti Kristjansson, "Deep adaptive AEC: Hybrid of deep learning and adaptive acoustic echo cancellation," in *Proc. ICASSP*, 2022, pp. 756–760.
- [9] Ross Cutler, Ando Saabas, Tanel Parnamaa, Marju Purin, Hannes Gamper, Sebastian Braun, Karsten Sørensen, and Robert Aichner, "ICASSP 2022 acoustic echo cancellation challenge," in *Proc. ICASSP*, 2022, pp. 9107–9111.
- [10] Jean-Marc Valin, Srikanth Tenneti, Karim Helwani, Umot Isik, and Arvinth Krishnaswamy, "Low-complexity, real-time joint neural echo control and speech enhancement based on percepnet," in *Proc. ICASSP*, 2021, pp. 7133–7137.
- [11] Ziteng Wang, Yueyue Na, Zhang Liu, Biao Tian, and Qiang Fu, "Weighted recursive least square filter and neural network based residual echo suppression for the AEC-challenge," in *Proc. ICASSP*, 2021, pp. 141–145.
- [12] Renhua Peng, Linjuan Cheng, Chengshi Zheng, and Xiaodong Li, "Acoustic echo cancellation using deep complex neural network with nonlinear magnitude compression and phase information," in *Proc. Interspeech*, 2021, pp. 4768–4772.
- [13] Feiran Yang, Gerald Enzner, and Jun Yang, "Frequency-domain adaptive Kalman filter with fast recovery of abrupt echo-path changes," *IEEE Signal Processing Letters*, vol. 24, pp. 1778–1782, 2017.
- [14] Gerald Enzner and Peter Vary, "Frequency-domain adaptive Kalman filter for acoustic echo control in hands-free telephones," *Signal Processing*, vol. 86, pp. 1140–1156, 2006.
- [15] Beren Millidge, Alexander Tschantz, Anil Seth, and Christopher Buckley, "Neural Kalman filtering," *arXiv preprint arXiv:2102.10021*, 2021.
- [16] Guy Revach, Nir Shlezinger, Xiaoyong Ni, Adria Lopez Escoriza, Ruud JG Van Sloun, and Yonina C Eldar, "Kalmannet: Neural network aided kalman filtering for partially known dynamics," *IEEE Transactions on Signal Processing*, vol. 70, pp. 1532–1547, 2022.
- [17] Huseyin Coskun, Felix Achilles, Robert DiPietro, Nassir Navab, and Federico Tombari, "Long short-term memory kalman filters: Recurrent neural estimators for pose regularization," in *Proc. of the IEEE International Conference on Computer Vision*, 2017, pp. 5524–5532.
- [18] Dong Yang, Fei Jiang, Wei Wu, Xuefei Fang, and Muyong Cao, "Low-complexity acoustic echo cancellation with neural Kalman filtering," *arXiv preprint arXiv:2207.11388*, 2022.
- [19] Wolfgang Mack and Emanuël AP Habets, "Deep filtering: Signal extraction and reconstruction using complex time-frequency filters," *IEEE Signal Processing Letters*, vol. 27, pp. 61–65, 2019.
- [20] Jonathan Le Roux, Scott Wisdom, Hakan Erdogan, and John R Hershey, "SDR—half-baked or well done?," in *Proc. ICASSP*, 2019, pp. 626–630.
- [21] Jiayu Du, Xingyu Na, Xuechen Liu, and Hui Bu, "AISHELL-2: Transforming mandarin ASR research into industrial scale," *arXiv:1808.10583*, 2018.
- [22] Jont B Allen and David A Berkley, "Image method for efficiently simulating small-room acoustics," *The Journal of the Acoustical Society of America*, vol. 65, pp. 943–950, 1979.
- [23] Gerald Enzner, Herbert Buchner, Alexis Favrot, and Fabian Kuech, "Acoustic echo control," in *Academic Press Library in Signal Processing*, vol. 4, pp. 807–877. 2014.
- [24] Antony W Rix, John G Beerends, Michael P Hollier, and Andries P Hekstra, "Perceptual evaluation of speech quality (PESQ) - A new method for speech quality assessment of telephone networks and codecs," in *Proc. ICASSP*, 2001, pp. 749–752.
- [25] "Tencent ASR," in <http://ai.qq.com/product/aaiasr.shtml>.